THE RELATIONSHIP BETWEEN RAMPART CRATER MORPHOLOGIES AND THE AMOUNT OF SUBSURFACE ICE. S. T. Stewart, J. D. O'Keefe, and Thomas J. Ahrens, Division of Geological and Planetary Sciences 150-21, California Institute of Technology, Pasadena, CA 91125, sstewart@gps.caltech.edu.

Introduction: Impact cratering on Earth, Mars, and icy satellites is significantly affected by the presence of subsurface H_2O. Martian rampart craters, characterized by the fluidized morphology of their ejecta blankets, are thought to form by impacts onto ice-rich areas [1]. We have been conducting experiments and modeling of impacts onto ice-rock mixtures to quantify the effects of subsurface H_2O on observable crater features, such as the ejecta distribution, rampart and pedestal formation, and crater floor morphologies. We find that the high volatility of H_2O modifies the crater formation process, resulting in more vapor production, higher ejection angles, fluidized ejecta blankets, and larger crater rim uplift. With our new insights into the crater formation process, the geographical distribution and morphology of fluidized ejecta blankets will constrain the amount of subsurface ice.

Cratering in Ice-Rich Materials: The presence of subsurface ice significantly alters the crater excavation process. Because ice is much more compressible than rock, about 4 times more energy is deposited in ice than rock at typical shock pressures. From our lab experiments, we find that ice will melt completely upon release from shock pressures ≥2-3 GPa, which is achieved in a zone of about 7 projectile radii (*Rp*)for asteroidal impacts on Mars.

Modification of crater excavation. We modeled impacts onto ice-rock mixtures under Martian conditions using the Eulerian finite difference code, CTH [2]. The simulations were initialized with a mixture of ice and rock in each cell, and separate equations of state were used for each component. The ejection angle is related to the strength of the material [3] and increases as the strength decreases. The angles are high and nearly constant in the zone (~7*Rp*) of water and brecciated rock, reaching nearly 70° for 20%vol subsurface ice, compared to a peak of ~60° in pure rock targets. In all cases, the ejection angles decreased to about 45° near the crater rim.

Properties of the ejected material. In the classical Z-model of crater excavation [4], streamtubes of material are ejected at constant angles with velocities that decrease from the impact point to the crater rim. Thus the material originally near the impact point travels ballistically to the outer ejecta blanket. Material is deposited from the crater rim outward, decreasing in thickness away from the crater rim.

The properties of ejected material at the time of ballistic emplacement are calculated using a Z-model modified to include the effects of ice. Fig. 1 shows the results for ejecta emplaced around a 10 km diameter crater in a 15%vol ice-rock mixture. For the rock-only case (solid lines), the ejection angles are approximately constant. The thickness of the blanket decreases with distance while the horizontal component of the velocity increases with radial distance. Note that the thickness of the ejected material, measured from the pre-existing surface level, is a lower limit since it does not include any porosity or entrainment of the surface material.

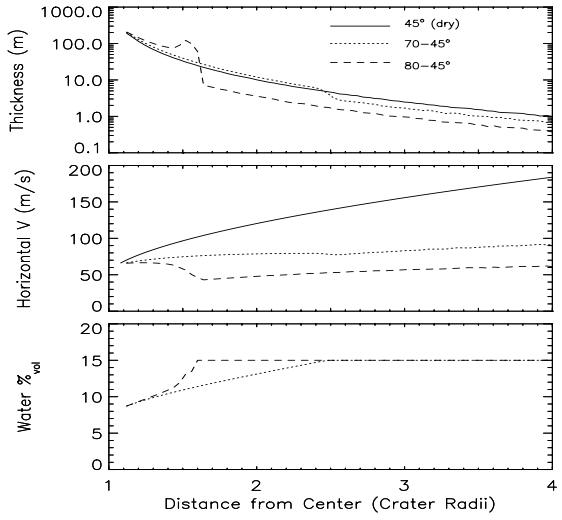

Fig. 1. Properties of ejected material at the time of ballistic emplacement around a 10 km diameter crater in a 15%vol ice-rock mixture.

When ice is present, the ejection angles are constant and steep in the zone where ice is melted and decrease toward the crater rim. This results in a knee in the thickness of the emplaced material that corresponds to the edge of the zone of water and brecciated rock. For peak ejection angles of 70°, which is consistent with 10-20%vol ground ice (Fig. 1a, dotted lines), the transition does not produce a large change in thickness (at 2.5 crater radii, *Rc*), but the horizontal velocities are more homogeneous and the water content is high. We suggest that, in this case, the presence of water and homogeneous flow velocities would allow the development of a single rampart in the ejecta blanket.

If the ejection angle is increased to 80°, e.g. for cases of even larger ice content (dashed lines), the

modification of the ejecta blanket is more pronounced, with a large step in the thickness of ejected material near 0.6 *Rc*. The flow velocities in this case may be slightly larger in the interior part of the blanket compared to the outer section which may allow for some overflowing onto the outer material. This situation may lead to a double rampart ejecta blanket.

The magnitude of the effects of the ejection angle transition increases with both increasing peak ejection angle and crater size. Higher ejection angles are indicative of a larger amount of subsurface ice.

Comparison to Mars Data: Fig. 2 presents the Mars Orbiter Laser Altimeter (MOLA) topography of a 10 km diameter rampart crater in northern polygonal terrain. The inner part of the ejecta blanket has a thickness of >100 m over the surrounding topography compared to 10's m in the outer ejecta blanket. The step in the thickness of the ejecta blanket occurs at about 2.5*Rc* from the center of the crater, similar to the 70^{o} ejection angle case (Fig. 1, dotted line). For a weak regolith, these ejection angles are consistent with our preliminary simulations of 10-20%vol ice content.

From our simulations, we find that the uplift of the crater rim is larger for impacts on ice-rock mixtures. The 10%vol ice-rock mixture uplift agrees very well with the observed crater rim topography (Fig. 2a). Ejecta are ballistically emplaced on top of the uplifted surface. The MOLA topography suggests that the ejecta has collected at the base of the uplifted area. The gray area shows the estimated thickness of ejecta accumulated from within the 12.5 km zone. The thickness of ejecta (a lower limit, since no porosity is included) agrees very well with the topography. With our model, the volume of the ejecta blanket is consistent with the crater formation process and does not require entrainment of additional material. To reach better agreement with the topography, this analysis would have to be combined with an estimate of the porosity of the material and the amount of post-emplacement flow.

In our model, the thick inner portion of the ejecta blanket contains less water than the outer ejecta blanket. Since the rheology of water-rock mixtures is very sensitive to the amount of water [5,6], the flow properties are probably very different in the inner vs. outer region. Thus, while the outer ejecta may be fluidized and flow long distances, in some cases, the inner ejecta may not flow significantly. In these situations, the location of the transition in the ejecta properties will be directly related to the amount of subsurface ice. The morphologies of rampart craters have previously been shown to be geographically correlated [7], supporting the relationship to subsurface ice. Using a range of crater sizes in a given geographical region, the size vs. morphology of rampart and pedestal craters may be used to infer the time-averaged amount of subsurface ice in the region. In general, the initial distal edge of the inner thick ejecta is located closer to the crater rim for higher ground ice content. Preliminary examination of pedestal craters on Ganymede and Europa support this formation hypothesis.

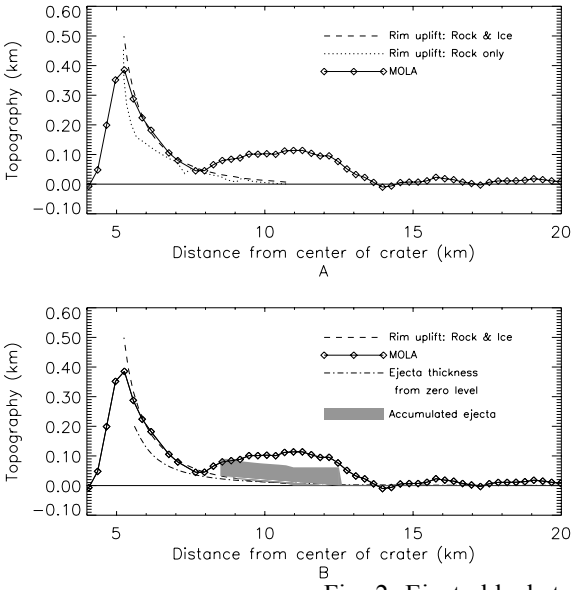

Fig. 2. Ejecta blanket of 10 km crater in polygonal terrain. The MOLA traverse coincides with MOC image M0901730.

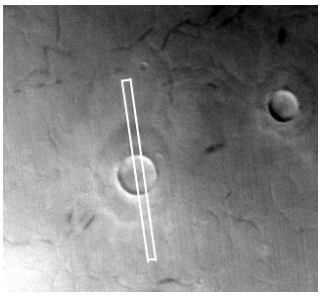

Fig. 3. Context image for MOLA data. MOC M0901731.

Conclusions: This analysis supports the hypothesis that rampart craters are formed because of the presence of subsurface ice. In the future, this cratering model, together with a model of post-emplacement flow, will be directly related to the amount of subsurface ice. We plan to use this model to investigate regional variability in the amount of subsurface H_2O on Mars.

Acknowledgements. We thank M. Lainhart and S. Byrne for computational assistance. This work was supported under NASA grant NAG5-8915.

References: [1] Carr M.H., et al. (1977) *JGR 82*, 4055-4065. [2] McGlaun JM, Thomson SL. (1990) *Int. J. Impact Eng. 10*, 360-361. [3] Melosh H.J. (1984) *Icarus 59*, 234-260. [4] Maxwell D.E. (1977) *Impact and Explosion Cratering*, 1003-1008. [5] Phillips C.J. and Davies R.H. (1991) *Geomorphology 4*,101-110. [6] Ivanov B.A. (1996). *Solar Sys. Res 30*, 43-58. [7] Barlow N.G. and Bradley T.L. (1990) *Icarus 87*, 156-179.